A Nature-Inspired Conjugated Polymer for High Performance Transistors and Solar Cells

Kealan J. Fallon,[†] Nilushi Wijeyasinghe,[‡] Nir Yaacobi-Gross,[‡] Raja S. Ashraf,[‡] David M. E. Freeman,[†] Robert G. Palgrave,[†] Mohammed Al-Hashimi,[§] Tobin J. Marks,[∥] Iain McCulloch,[‡] Thomas D. Anthopoulos,[‡] and Hugo Bronstein*,[†]

[†]Department of Chemistry, University College London, Christopher Ingold Building, London WC1H 0AJ, U.K.

[‡]Centre for Plastic Electronics, Imperial College London, London SW7 2AZ, U.K.

[§]Department of Chemistry, Texas A&M University at Qatar, P.O. Box 23874, Doha, Qatar

[∥]Department of Chemistry, Materials Research Center, and Argonne-Northwestern Solar Energy Research Center, Northwestern University, 2145 Sheridan Road, Evanston, Illinois 60208, United States

S Supporting Information

ABSTRACT: A novel, highly soluble chromophore for use in organic electronics based on an indigoid structure is reported. Copolymerization with thiophene affords an extremely narrow band gap polymer with a maximum absorption at ~800 nm. The novel polymer exhibits high crystallinity and high ambipolar transport in OFET devices of 0.23 cm^2 V^{-1} s^{-1} for holes and 0.48 cm^2 V^{-1} s^{-1} for electrons. OPV device efficiencies up to 2.35% with light absorbance up to 950 nm demonstrate the potential for this novel chromophore in near-IR photovoltaics.

μ_{hole} = 0.23 cm^2/Vs
$\mu_{electron}$ = 0.48 cm^2/Vs

nature-inspired precursor

λ_{max} = 797 nm
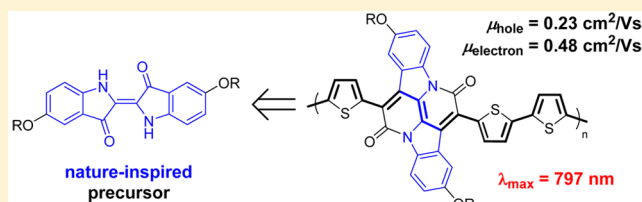
INTRODUCTION

The development of novel organic conjugated polymers has gained momentum in recent times due to their possible applications in organic photovoltaic (OPV) and organic field-effect transistor (OFET) devices where their lower cost, light weight, and mechanical flexibility are all attractive properties. Current high performance polymers have enabled OFET devices with mobilities in excess of 2 cm^2 V^{-1} s^{-1} and OPV devices with power conversion efficiencies (PCEs) of over 8%.[1−3] Ultra-narrow band gap conjugated polymers are of great interest due to the ease of charge injection when incorporated into ambipolar OFETs and also their near-IR optical absorption for use in both tandem and transparent OPV devices.[4] Considerable interest has focused on planar bis-lactam containing polymers such as diketopyrrolopyrrole (DPP, **1**)[5] and isoindigo (**2**).[6] The electron withdrawing nature of the lactam core alongside its planarity has enabled DPP and isoindigo containing conjugated polymers to reach both OPV PCEs and OFET mobilities.

Indigo (**3**) is the most produced natural dye worldwide and has a highly planar structure arising from intramolecular hydrogen bonding between the oxygen and the amide protons of the indol-3-one units.[7] Upon photoexcitation, rotation about the central carbon−carbon bond can effect *trans*−*cis* isomerization[8] as well as either single or double proton transfer, resulting in rapid energy loss through internal conversion, thereby negating any potential for OPV devices.[9] As a semiconductor in OFET devices, indigo has shown hole mobilities up to 1 × 10^{-2} cm^2 V^{-1} s^{-1}.[10] More recently,
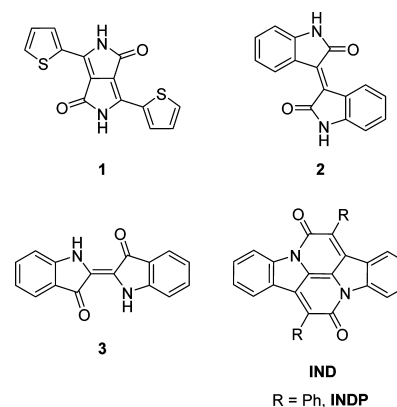

Figure 1. Bis-lactam containing compounds and polymer building blocks.

functionalized indigoids have been investigated, and the mobility can be slightly enhanced to 1.3 × 10^{-2} cm^2 V^{-1} s^{-1} using 5,5′-dichloroindigo.[11] Crucially, the use of naturally occurring compounds as building blocks for materials in organic electronics can begin to address the issues of sustainability associated with them. As an example, Cibalackrot (7,14-diphenyldiindolo[3,2,1-*de*:3′,2′,1′-*ij*][1,5]naphthyridine-6,13-dione, INDP) is an indigo derivative first synthesized in

Scheme 1. Synthetic Route to the Novel INDT Monomer
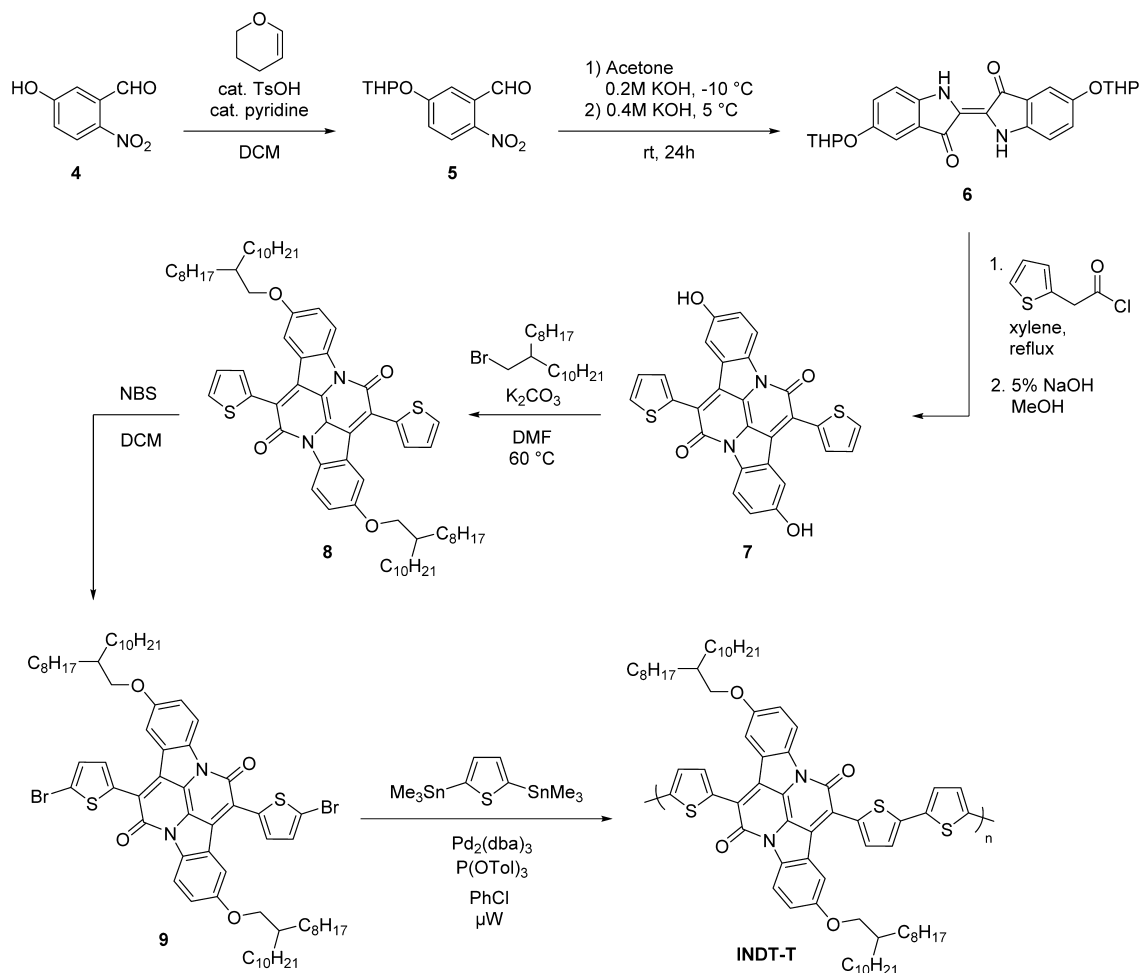
Table 1. Physical and Optical Properties of INDT-T

$M_n{}^a$	$M_w{}^a$	PDI^a	λ_{max}^{soln} (nm)^b	λ_{max}^{film} (nm)^c	HOMO (eV)^d	LUMO (eV)^e	E_g (eV)^c	E_g^{calc} (eV)^f
15700	49400	3.15	797	790	−4.24	−3.02	1.22	1.32

^{a}Determined by SEC(PS) using PhCl as eluent. ^{b}PhCl solution. ^{c}Spin-coated from PhCl 5 mg/mL. ^{d}Determined by XPS. ^{e}HOMO + optical energy gap. ^{f}Determined by TD-DFT using B3LYP/6-31g*.

1914 by condensation of indigo and phenylacetyl chloride.[12] Importantly, the molecule is locked in a highly planar rigid conformation where proton transfer and *trans–cis* isomerization are not possible. This highly conjugated compound has similar functionality to compounds containing the popular bis-lactam system, and hence polymers based on this structure display interesting electronic properties. Remarkably, however, there are almost no reports of IND implementation in organic electronics. Glowacki et al. reported the use of the parent small molecule in OFET devices to obtain reasonable OFET mobilities,[13] and very recently He et al. demonstrated its use as a comonomer to achieve high field effect mobilities when copolymerized with solubilizing comonomers.[14] We were interested in developing soluble IND derivatives which would not require copolymerization with complex comonomers, and here we report the first synthesis of such materials and their potential for use in organic electronics. By demonstrating the use of conjugated polymers containing naturally occurring and potentially biosustainable building blocks, we believe that we

are taking important steps toward addressing the issue of sustainability in organic electronics.

■ **RESULTS AND DISCUSSION**

The synthesis (Scheme 1) begins with protection of commercially available 5-hydroxy-2-nitrobenzaldehyde (**4**) with 3,4-dihydro-2H-pyran, followed by an aldol condensation to give (E)-5,5′-bis((tetrahydro-2H-pyran-2-yl)oxy)-[2,2′-biin-dolinylidene]-3,3′-dione (**6**). A subsequent condensation reaction and concurrent deprotection of the tetrahydropyranyl groups affords the 2,9-dihydroxy-7,14-di(thiophen-2-yl)-diindolo[3,2,1-de:3′,2′,1′-ij][1,5]naphthyridine-6,13-dione (INDT) compound **7**. This compound was then alkylated with 2-octyldodecyl chains to improve solubility and then subsequently brominated with N-bromosuccinimide to afford our novel INDT monomer **9**. Copolymerization via Stille coupling of monomer **9** with simple bis(trimethylstannyl)-thiophene affords polymer INDT-T, which was purified by Soxhlet extraction using acetone, then hexane, to remove low molecular weight oligomers, and finally chloroform. The dark

green polymeric product is soluble in common organic solvents such as chloroform and chlorobenzene.

The molecular mass of INDT-T was determined by SEC(PS) to be $M_n \sim 15.7$ kDa and $M_w \sim 49.4$ kDa which, although is perhaps lower than optimal, is sufficient to evaluate the promise of this material in organic electronic devices. Figure 2a shows the solution (chlorobenzene) and thin film (spin-
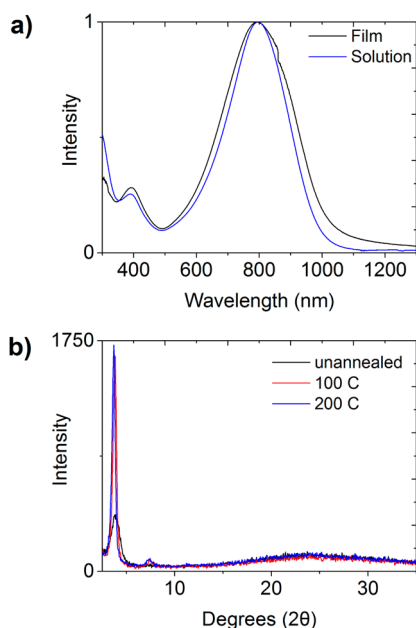

Figure 2. (a) Normalized UV−vis absorption spectra of INDT-T. Solution spectra were recorded in chlorobenzene, and thin films were spun from a 5 mg/mL solution of INDT-T in chlorobenzene. (b) X-ray diffraction of a drop-cast INDT-T film from a 5 mg/mL solution of INDT-T in chlorobenzene.

coated from a 5 mg/mL solution in chlorobenzene) UV−vis absorption spectra of INDT-T. Both spectra show a broad featureless absorption in the near-IR with $\lambda_{max} \sim 790$ nm. The spectrum becomes somewhat broadened on going from solution to thin films which is attributed to solid state packing effects, often observed in similar materials. The optical band gap in the film can be estimated to be ~ 1.22 eV, demonstrating the effectiveness of the IND core at creating near-IR-absorbing materials. The HOMO and LUMO energy levels were determined by XPS, and the optical energy gaps are found to be −4.24 and −3.02 eV, respectively. Both values are in a similar range to typical DPP and isoindigo polymers, thus showing that the IND containing polymers are an important addition to the bis-lactam containing conjugated polymer family.

The influence of annealing temperature on the molecular packing in INDT-T thin films was studied by X-ray diffraction (Figure 2b). Drop-cast polymer thin films (5 mg/mL solution in chlorobenzene) show a Bragg reflection at $2\theta = 3.8°$, corresponding to the (100) reflection and indicative of a typical lamellar packing distance of 2.3 nm. Annealing at 100 °C for 10 min leads to a substantial increase in thin film crystallinity as observed by the increased intensity of the (100) peak, though we note that this improvement may not necessarily arise from increased ordering of the π−π stacking in the thin film.[15] The appearance of the corresponding (200) reflection also indicates increased long-range order. No noticeable changes in the film crystallinity are observed after annealing at higher temperatures.

To investigate the electronic structure of the new polymer, DFT calculations were carried out on model trimers with methoxy substituents. The calculated energy gap is found to be 1.32 eV, in good agreement with experiment. Figure 3 shows the HOMO and LUMO distributions of the geometry optimized structure of INDT-T using Gaussian 09 (DFT, B3LYP/6-31G*). The backbone displays a high degree of
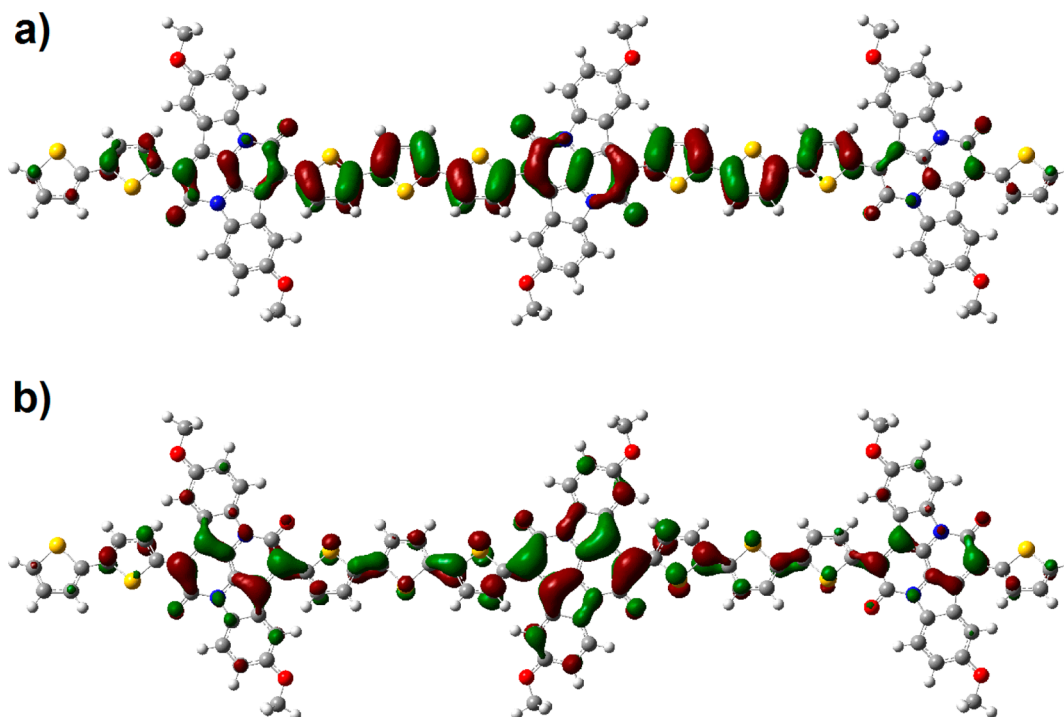

Figure 3. (a) HOMO and (b) LUMO distributions of the geometry-optimized structure of INDT-T using Gaussian 09 (DFT, B3LYP/6-31G*).

coplanarity indicating that charge transport in this material should be efficient. Both the HOMO and LUMO are delocalized well over both the thiophenes and the central bislactam core. However, while there is little contribution to the HOMO from the peripheral phenyl groups, there is substantial delocalization of the LUMO onto these sites. This indicates that further substitutions at these positions will enable independent manipulation of the LUMO level without disruption of the HOMO.

OFETs with top gate−bottom contact architecture were fabricated using the novel polymer on glass substrates with CYTOP dielectric. Al + Au bilayer (20 nm + 20 nm) electrodes for ambipolar charge transport were used. The organic semiconductor layer was spin-coated on top of the substrates from a chlorobenzene solution (10 mg/mL). Finally, CYTOP dielectric was spin-coated on top followed by a thermally evaporated Al gate electrode. Representative transfer and output characteristics are shown in Figure 4, and data are
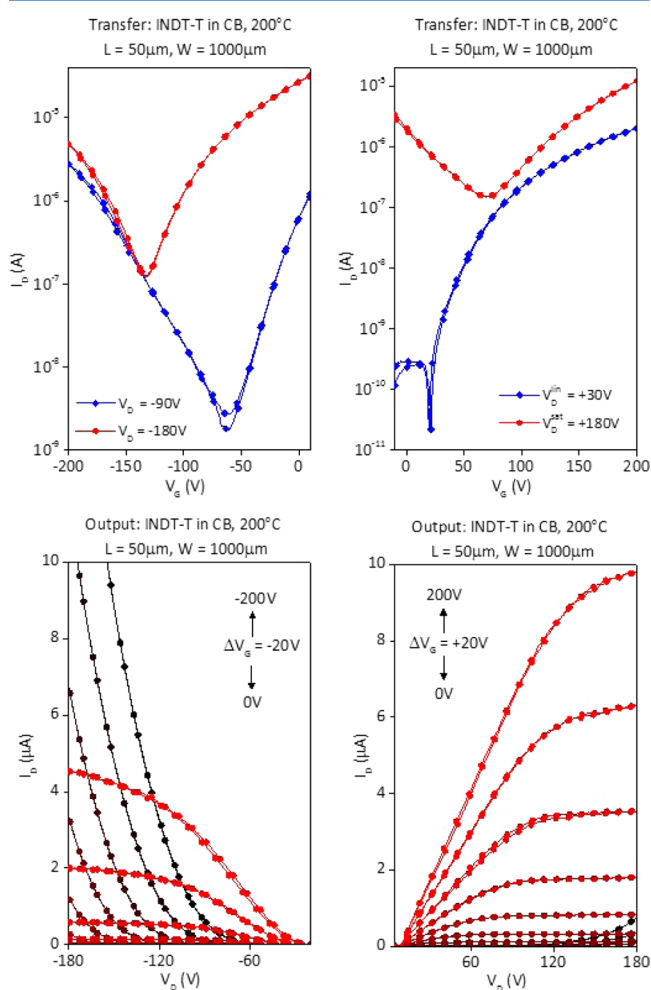

Figure 4. Transfer and output characteristics of an OFET devices of INDT-T annealed at 200 °C.

compiled in Tables 2 and 3. The 100 °C annealed film maximum hole and electron mobilities extracted from the saturation regime of the transfer curves are both approximately 0.08 cm^2 V^{-1} s^{-1}, demonstrating good balanced ambipolar behavior and negligible hysteresis. Annealing the devices at 200 °C leads to significant improvement in both the hole and electron mobility. A high hole mobility of 0.23 cm^2 V^{-1} s^{-1} is

determined from the best fit of the second derivative of transfer curve saturation regime with the peak value measured being 0.52 cm^2 V^{-1} s^{-1}. The best-fit value for the electron mobility is 0.48 cm^2 V^{-1} s^{-1} with a remarkable peak mobility of 1.2 cm^2 V^{-1} s^{-1}; however, we note that there was a significant amount of noise present in the second-derivative mobility extraction plot. As was shown in XRD experiments, we believe that the improved OFET characteristics are due to the increased ordering of the INDT-T polymer with annealing.

The threshold voltage for electrons is in the range of ~20−50 V which is comparable to values measured in DPP and isoindigo-based OFETs. However, the large threshold voltages for holes indicate an injection barrier. We attribute this to nonoptimized matching of the electrodes and the polymer HOMO. To overcome this, OFETs with UV-O$_3$-treated Au electrodes with an Al adhesion layer (40 + 5 nm) for optimized hole injection due to a deeper work function were fabricated. The results are shown in Table 3.

Only p-type transport is observed for these devices; however, it is clear that both the measured hole mobility and threshold voltage are significantly improved relative to the equivalent devices presented in Table 2. This indicates that the larger threshold voltages observed in the initial device data are likely due to improper work function matching or suboptimal metal−polymer contact. Bottom gate−bottom contact OFET devices were also fabricated, but these suffered from significant hysteresis and lower mobilities.

Conventional and inverted bulk-heterojunction OPV devices were fabricated using a 1:2 blend of INDT-T:PC$_{71}$BM as the active layer spin-coated from a 4:1 CHCl$_3$:ODCB solution (10 mg/mL). The J−V curves and EQE are shown in Figure 5, and the data are presented in Table 4. The conventional OPV device provides a PCE of 2.25%, with a short circuit current (J_{sc}) of 6.27 mA cm^{-2}, an open circuit voltage (V_{oc}) of 0.62 V, and a fill factor (FF) of 0.58. The relatively high open circuit voltage is impressive considering the extremely narrow band gap of INDT-T, and the devices all have relatively good fill factors, indicating good charge extraction at low fields. The inverted devices show similar overall efficiencies of 2.35% but have slightly increased short circuit currents (J_{sc} = 6.88 mA cm^{-2}) and lower open circuit voltages (V_{oc} = 0.59 V). Similar variations between conventional and inverted OPV devices have been shown before in DPP-based conjugated polymers. The EQE shows that the majority of the photocurrent originates from the fullerene absorption, but there remains an appreciable contribution from the extremely near-IR absorbing INDT-T polymer up to 950 nm. Despite the modest overall efficiencies, these devices represent some of the highest efficiencies from such ultranarrow band gap materials.[16] We believe that the lower contribution to the photocurrent is predominantly due to insufficient energetic offset of the polymer with respect to the fullerene.[17] More importantly, we demonstrate the first functioning OPV devices of this very novel chromophore, indicating that it is well-suited for further development in this field.

■ CONCLUSION

We report the synthesis of a novel soluble monomer INDT for use in conjugated polymers based on naturally occurring indigo. Incorporation of this novel unit in a conjugated polymer, INDT-T, results in an extremely narrow band gap material with high crystallinity. This polymer exhibits high ambipolar transport in OFET devices, with holes and electrons exhibiting

Table 2. OFET Characteristics of INDT-T

annealing temp (°C)	channel length (μm)	$\mu_{hole}{}^{a,b}$ (peak value) (cm^2 V^{-1} s^{-1})	$V_{th,hole}{}^{c}$ (V)	I_{on}/I_{off} for holes^{c}	$\mu_{electron}{}^{a,b}$ (peak value) (cm^2 V^{-1} s^{-1})	$V_{th,electron}{}^{c}$ (V)	I_{on}/I_{off} for electrons^{c}
100	40	0.04 ± 0.003^{d} (0.046 ± 0.002)	−120 ± 8	10^4	0.075 ± 0.01 (0.11 ± 0.03)	43 ± 5	10^5
	50	0.076 (0.09)	−23	10^5	0.075 (0.094)	22	10^6
	100	0.048 (0.069)	−90	10^5	0.079 (0.13)	29	10^6
200	50	0.23 ± 0.01^{e} (0.52 ± 0.08)	−131 ± 2	10^3	0.48 ± 0 (1.2 ± 0.05)	52 ± 3	10^6

$^{a}\mu_{hole}$ and $\mu_{electron}$ refer to the highest effective mobilities measured in the saturation regime for a gate-voltage range of 20 V. ^{b}Peak values for saturation regime mobility are given in parentheses next to the best-fit values because the second-derivative plots are noisier. ^{c}The threshold voltages (V_{th}) and the on-to-off ratios (I_{on}/I_{off}) were extracted from the linear regime (V_d = −30 V (all devices) except for 200 °C annealed (−90 V) for holes and V_d = 30 V (all devices) except for 40 μm device (60 V) for electrons). ^{d}Average of four devices. ^{e}Average of two devices.

Table 3. Hole Optimized OFET Characteristics of INDT-T

annealing temp (°C)	channel length (μm)	$\mu_{hole}{}^{a,b}$ (peak value) (cm^2 V^{-1} s^{-1})	$V_{th,hole}{}^{c}$ (V)	I_{on}/I_{off} for holes^{c}
100	30	0.1 ± 0.01^{d} (0.13 ± 0.015)	−14 ± 0.5	10^4

$^{a}\mu_{hole}$ refers to the highest effective mobilities measured in the saturation regime for a gate-voltage range of 20 V. ^{b}Peak values for saturation regime mobility are given in parentheses next to the best-fit values because the second-derivative plots are noisier. ^{c}The threshold voltages (V_{th}) and the on-to-off ratios (I_{on}/I_{off}) were extracted from the linear regime (V_d = −30 V) for holes. ^{d}Average of two devices.
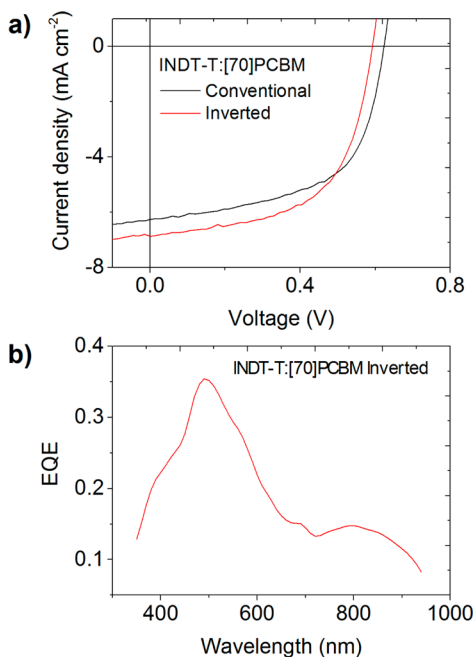

Figure 5. (a) $J-V$ characteristics of INDT-T:PC[70]BM solar cells. (b) External quantum efficiency of the INDT-T:PC[70]BM solar cell.

Table 4. OPV Device Characteristics of INDT-T-Based Solar Cells

architecture	J_{sc} (mA cm^{-2})	V_{oc} (V)	FF	PCE (%)
conventional	6.27	0.62	0.58	2.25
inverted	6.88	0.59	0.58	2.35

mobilities of 0.23 and 0.48 cm^2 V^{-1} s^{-1}, respectively. Conventional and inverted OPV devices give efficiencies of up to 2.35% with photocurrent generated up to 950 nm, demonstrating the potential of this novel monomer unit for implementation in near-IR OPV devices.

■ EXPERIMENTAL SECTION

Characterization. ^{1}H NMR spectra were recorded at 400 MHz on a Bruker Avance 400 spectrometer, at 500 MHz on a Bruker Avance 500 spectrometer, or at 600 MHz on a Bruker Avance 600 spectrometer in the stated solvent using residual protic solvent CHCl$_3$ (δ = 7.26 ppm, s) or DMSO (δ = 2.56 ppm, qn) as the internal standard. ^{13}C NMR spectra were recorded at 125 MHz on a Bruker Avance 500 spectrometer or at 150 MHz on a Bruker Avance 600 spectrometer in the stated solvent using the central reference of CHCl$_3$ (δ = 77.0 ppm, t) or DMSO (δ = 39.52 ppm, septet) as the internal standard. Mass spectra were obtained using either a VG70-SE or MAT 900XP spectrometer at the Department of Chemistry, University College London. X-ray diffraction (XRD) measurements were carried out with a Bruker D4 Endeavor diffractometer equipped with a nickel-filtered Cu Kα_1 beam and a scintillation counter detector and postsample graphite monochromator, using a current of 30 mA and an accelerating voltage of 40 kV. UV−vis spectra were recorded on a PerkinElmer Lambda 950 spectrophotometer.

Synthesis. *2-Nitro-5-((tetrahydro-2H-pyran-2-yl)oxy)-benzaldehyde.* 5-Hydroxy-2-nitrobenzaldehyde (5.09 g, 31 mmol) and 3,4-dihydro-2H-pyran (13.7 mL, 0.15 mol) were dissolved in a 4:1 solution of dichloromethane:hexane (61 mL). *p*-Toluenesulfonic acid (58 mg, 1 mol %) was suspended in dichloromethane (15 mL), and a few drops of pyridine were added. The acidic mixture was then added in one portion, and the reaction was stirred for 12 h. Solvent and unreacted 3,4-dihydro-2H-pyran were then removed *in vacuo* to give a brown oil which was purified by flash chromatography on silica gel (4:1, PET:EtOAc, R_F = 0.3) to give the product as a yellow oil (7.66 g, 100%). ^{1}H NMR (400 MHz, CDCl$_3$) δ: 10.49 (s, 1H), 8.17 (d, J = 9.0 Hz, 1H), 7.51 (d, J = 2.8 Hz, 1H), 7.33 (dd, J = 9.0, 2.8 Hz, 1H), 5.62 (t, J = 2.8 Hz, 1H), 3.84−3.74 (m, 1H), 3.71−3.63 (m, 1H), 1.96−1.90 (m, 2H), 1.80−1.69 (m, 2H), 1.68−1.62 (m, 2H). LRMS (CI+) *m/z* 252 [MH]$^+$.

(E)-5,5′-Bis(benzyloxy)-[2,2′-biindolinylidene]-3,3′-dione. 2-Nitro-5-((tetrahydro-2H-pyran-2-yl)oxy)benzaldehyde (2.3 g) was dissolved in acetone (34.5 mL) and cooled to −10 °C. With vigorous stirring, a 0.2 M solution of potassium hydroxide (4.6 mL) was added dropwise over 15 min, turning the solution pale yellow. After 30 min the solution was warmed to 5 °C, and a 0.4 M solution of potassium hydroxide (34.5 mL) was added dropwise slowly. When half of this solution was added, the reaction turned deep green; once addition was complete, the reaction was a dark green/blue color. After addition, the reaction was covered and allowed to warm to room temperature and stirred for 24 h. The solid was then collected by vacuum filtration and washed with methanol until washings ran colorless to give a blue solid

(0.72 g, 34%). ^{1}H NMR (600 MHz, CDCl$_3$) δ: 8.76 (s, 2H), 7.42 (d, J = 2.5 Hz, 2H), 7.22 (dd, J = 8.7, 2.5 Hz, 2H), 6.96 (d, J = 8.7 Hz, 2H), 5.34 (t, J = 3.3 Hz, 2H), 3.97−3.88 (m, 2H), 3.68−3.58 (m, 2H), 2.04−1.94 (m, 4H), 1.92−1.82 (m, 4H), 1.73−1.63 (m, 4H). LRMS (CI+): m/z 463 [MH]$^+$. HRMS Found (CI+): [MH]$^+$ 463.18632; C$_{26}$H$_{27}$N$_2$O$_6$ requires 463.18691.

2,9-Dihydroxy-7,14-di(thiophen-2-yl)diindolo[3,2,1-de:3′,2′,1′-ij]-[1,5]naphthyridine-6,13-dione. (*E*)-5,5′-Bis((tetrahydro-2*H*-pyran-2-yl)oxy)-[2,2′-biindolinylidene]-3,3′-dione (2.2 g, 4.8 mmol), and 2-(thiophen-2-yl)acetyl chloride (3.6 mL, 29 mmol) were dissolved in anhydrous xylene (96 mL), and the reaction refluxed at 165 °C for 24 h. The blue reaction turned purple after 1 h. After 24 h the vapors from the argon flow were no longer acidic. The reaction was transferred to a 250 mL round-bottomed flask washing with methanol and chloroform. All solvent was removed *in vacuo* to give a black residue. The residue was taken up in methanol, and the yellow methanol washings carefully decanted off, to leave the black solid in the flask. After five methanol washings the solid was suspended in methanol, and with stirring, 5% sodium hydroxide solution (20 mL, 2.5 equiv) was added. The solution immediately turned dark red and then black and allowed to stir for 12 h. 6 M hydrochloric acid (4.1 mL, 24.8 mmol) was then added to neutralize the reaction. The methanol and water were then removed *in vacuo*, and the resulting residue was washed with a small amount of water which was carefully decanted off to remove any salts. The solid was then taken up in acetone and filtered off under reduced pressure. The resulting dark solid was washed with water, acetone, and then methanol and air-dried to give a black solid (0.7 g, 29%). ^{1}H NMR (600 MHz, DMSO) δ: 10.03 (s, 2H), 8.22 (d, J = 8.7 Hz, 2H), 7.96 (d, J = 4.5 Hz, 2H), 7.74 (d, J = 3.6 Hz, 2H), 7.53 (d, J = 2.4 Hz, 2H), 7.35 (dd, J = 4.5, 3.6 Hz, 2H), 7.07 (dd, J = 8.7, 2.4 Hz, 2H). LRMS (ES+) m/z 507 [MH]$^+$. HRMS Found (ES+): [MH]$^+$ 507.0482; C$_{28}$H$_{15}$N$_2$O$_4$S$_2$ requires 507.0473.

2,9-Bis((2-octyldodecyl)oxy)-7,14-di(thiophen-2-yl)diindolo[3,2,1-de:3′,2′,1′-ij][1,5]naphthyridine-6,13-dione. 2,9-Dihydroxy-7,14-di-(thiophen-2-yl)diindolo[3,2,1-*de*:3′,2′,1′-*ij*][1,5]naphthyridine-6,13-dione (0.7 g, 1.4 mmol), potassium carbonate (2.67 g, 19 mmol), and 9-(bromomethyl)nonadecane (1.25 g, 3.5 mmol) were dissolved in dimethylformamide (28 mL) and heated at 60 °C with stirring for 24 h. The reaction was then cooled and poured into a separating funnel containing brine and hexane. The organic layer was extracted with brine (5 × 50 mL), separated, and filtered under reduced pressure to remove black particulates. The purple organic filtrate was then dried over magnesium sulfate, filtered, and concentrated *in vacuo* to give a purple oil. The crude oil was purified by flash chromatography on silica gel (9:1, PET: EtOAc, R_F = 0.2) to give a pure purple oil (119 mg, 8%). ^{1}H NMR (600 MHz, CDCl$_3$) δ: 8.40 (d, J = 8.9 Hz, 2H), 7.74 (dd, J = 3.6, 0.8 Hz, 2H), 7.69 (dd, J = 5.1, 0.8 Hz, 2H), 7.65 (d, J = 2.5 Hz, 2H), 7.27−7.24 (m, 2H), 7.08 (dd, J = 8.9, 2.5 Hz, 2H), 3.81 (d, J = 5.8 Hz, 4H), 1.81−1.73 (m, 2H), 1.47−1.40 (m, 4H), 1.40−1.35 (m, 4H), 1.35−1.20 (m, 56H), 0.90−0.84 (m, 12H). ^{13}C NMR (150 MHz, CDCl$_3$) δ: 158.5, 158.0, 138.0, 134.8, 130.3, 130.2, 130.1, 127.1, 126.3, 125.1, 122.5, 118.4, 118.3, 111.0, 71.9, 38.0, 32.0, 31.4, 30.2, 29.8, 29.7, 29.5, 26.9, 22.8, 14.3. LRMS (ES−) m/z 1065 [M − H]$^+$.

7,14-Bis(5-bromothiophen-2-yl)-2,9-bis((2-octyldodecyl)oxy)-diindolo[3,2,1-de:3′,2′,1′-ij][1,5]naphthyridine-6,13-dione. 2,9-Bis-((2-octyldodecyl)oxy)-7,14-di(thiophen-2-yl)diindolo[3,2,1-*de*:3′,2′,1′-*ij*][1,5]naphthyridine-6,13-dione (119 mg, 0.11 mmol) was dissolved in dichloromethane (15 mL), and the solution was cooled to 0 °C. *N*-Bromosuccinimide (43 mg, 0.24 mmol) was added all at once to the stirring solution, and the reaction was covered and kept at 0 °C for 30 min. The ice bath was then removed, and the reaction was allowed to warm to room temperature and stir for a further 12 h. After 1 h the solution had changed from purple to sapphire blue. After 12 h, the reaction was diluted with further dichloromethane, washed with water (2 × 30 mL) and then brine (30 mL), dried over magnesium sulfate, and concentrated to give a waxy solid. Methanol was added to the flask and to give a suspension, which was then collected by vacuum filtration to give a pure blue waxy solid (60 mg, 44%). ^{1}H NMR (600 MHz, CDCl$_3$) δ: 8.34 (d, J = 8.9 Hz, 2H), 7.67 (d, J = 2.4 Hz, 2H),

7.54 (d, J = 3.9 Hz, 2H), 7.21 (d, J = 3.9 Hz, 2H), 7.07 (dd, J = 8.9, 2.4 Hz, 2H), 3.83 (d, J = 5.7 Hz, 4H), 1.83−1.75 (m, 2H), 1.48−1.41 (m, 4H), 1.41−1.36 (m, 4H), 1.36−1.17 (m, 56H), 0.91−0.83 (m, 12H). ^{13}C NMR (150 MHz, CDCl$_3$) δ: 158.1, 137.6, 136.6, 123.0, 129.2, 129.0, 126.8, 124.4, 122.4, 118.7, 111.0, 72.0, 51.0, 38.0, 32.0, 31.4, 30.2, 29.8, 29.5, 27.0, 22.8, 14.3. HRMS Found (ES−): [M − H]$^-$ 1221.4817; C$_{68}$H$_{91}$Br$_2$N$_2$O$_4$S$_2$ requires 1221.4787.

Polymer INDT-T. 7,14-Bis(5-bromothiophen-2-yl)-2,9-bis((2-octyldodecyl)oxy)diindolo[3,2,1-*de*:3′,2′,1′-*ij*][1,5]naphthyridine-6,13-dione (60.1 mg, 49.1 μmol), tris(dibenzylideneacetone)dipalladium(0) (2.6 mg, 2.8 μmol, 6 mol %), tri(*o*-tolyl)phosphine (3.47 mg, 11.4 μmol), and 2,5-bis(trimethylstannyl)thiophene (20.15 mg, 49.1 μmol) were added to a dry 10 mL microwave vial equipped with a stirrer bar and sealed. Chlorobenzene (2.5 mL) was added via syringe, and the solution was degassed with argon for 30 min. The vial was then placed in a microwave reactor and heated as follows: 10 min at 100 °C, 5 min at 120 °C, 5 min at 140 °C, 5 min at 160 °C, and 20 min at 180 °C. The vial was then allowed to cool, and the reaction had changed color from sapphire blue to turquoise. The reaction mixture was added dropwise slowly into rapidly stirring methanol (70 mL) and allowed to stir for 2 h, forming fine dark blue fibers. The polymeric material was then filtered under reduced pressure into a cellulose thimble and washed with methanol and then acetone. The polymer was purified by Soxhlet extraction as follows: acetone for 12 h, hexane for 12 h, and chloroform for 12 h. The chloroform was then concentrated to give a turquoise plastic-like film on the round-bottomed flask. This film was dissolved in a minimum volume of hot chlorobenzene (∼2.5 mL) and then added dropwise slowly into rapidly stirring methanol cooled to 0 °C. Once addition was complete, the methanol was stirred for 30 min, filtered under vacuum, washed carefully with methanol and then a small amount of acetone, then allowed to dry, forming a dark blue film. The polymer was air-dried for 1 h, placed in a vial, and dried under vacuum for 12 h (49 mg, 87%). GPC (PS): M_n = 15687, M_w = 49381, PDI = 3.15. UV (PhCl) λ_{max} 797, (thin film) λ_{max} 790.

■ ASSOCIATED CONTENT

Ⓢ Supporting Information

Experimental details, characterizations, and NMR spectra. The Supporting Information is available free of charge on the ACS Publications website at DOI: 10.1021/acs.macromol.5b00542.

■ AUTHOR INFORMATION

Corresponding Author

*E-mail: h.bronstein@ucl.ac.uk (H.B.).

Notes

The authors declare no competing financial interest.

■ ACKNOWLEDGMENTS

■ REFERENCES

(1) Bronstein, H.; Chen, Z.; Ashraf, R. S.; Zhang, W.; Du, J.; Durrant, J. R.; Shakya Tuladhar, P.; Song, K.; Watkins, S. E.; Geerts, Y.; Wienk, M. M.; Janssen, R. A. J.; Anthopoulos, T.; Sirringhaus, H.; Heeney, M.; McCulloch, I. *J. Am. Chem. Soc.* **2011**, *133* (10), 3272−3275.

(2) Zhang, X.; Bronstein, H.; Kronemeijer, A. J.; Smith, J.; Kim, Y.; Kline, R. J.; Richter, L. J.; Anthopoulos, T. D.; Sirringhaus, H.; Song, K.; Heeney, M.; Zhang, W.; McCulloch, I.; DeLongchamp, D. M. *Nat. Commun.* **2013**, *4*, 2238.

(3) Guo, X.; Zhou, N.; Lou, S. J.; Smith, J.; Tice, D. B.; Hennek, J. W.; Ortiz, R. P.; Navarrete, J. T. L.; Li, S.; Strzalka, J.; Chen, L. X.; Chang, R. P. H.; Facchetti, A.; Marks, T. J. *Nat. Photonics* **2013**, *7* (10), 825−833.

(4) Li, W.; Hendriks, K. H.; Roelofs, W. S. C.; Kim, Y.; Wienk, M. M.; Janssen, R. A. J. *Adv. Mater.* **2013**, *25* (23), 3182−3186.

(5) Naik, M. A.; Patil, S. *J. Polym. Sci., Part A: Polym. Chem.* **2013**, *51* (20), 4241−4260.

(6) Deng, P.; Zhang, Q. *Polym. Chem.* **2014**, *5* (10), 3298−3305.

(7) Guo, C.; Sun, B.; Quinn, J.; Yan, Z. Q.; Li, Y. N. *J. Mater. Chem. C* **2014**, *2* (21), 4289−4296.

(8) Gorner, H.; Pouliquen, J.; Kossanyi, J. *Can. J. Chem.* **1987**, *65* (4), 708−717.

(9) Rondão, R.; Seixas de Melo, J.; Melo, M. J.; Parola, A. J. *J. Phys. Chem. A* **2012**, *116* (11), 2826−2832.

(10) Irimia-Vladu, M.; Głowacki, E. D.; Troshin, P. A.; Schwabegger, G.; Leonat, L.; Susarova, D. K.; Krystal, O.; Ullah, M.; Kanbur, Y.; Bodea, M. A.; Razumov, V. F.; Sitter, H.; Bauer, S.; Sariciftci, N. S. *Adv. Mater.* **2012**, *24* (3), 375−380.

(11) Klimovich, I. V.; Leshanskaya, L. I.; Troyanov, S. I.; Anokhin, D. V.; Novikov, D. V.; Piryazev, A. A.; Ivanov, D. A.; Dremova, N. N.; Troshin, P. A. *J. Mater. Chem. C* **2014**, *2*, 7621.

(12) Engi, G. Z. *Angew. Chem.* **1914**, *27*, 144.

(13) Glowacki, E. D.; Leonat, L.; Voss, G.; Bodea, M.; Bozkurt, Z.; Irimia-Vladu, M.; Bauer, S.; Sariciftci, N. S. In *Natural and Nature-Inspired Semiconductors for Organic Electronics*, 2011; pp 81180M-81180M−10.

(14) He, B.; Pun, A. B.; Zherebetskyy, D.; Liu, Y.; Liu, F.; Klivansky, L. M.; McGough, A. M.; Zhang, B. A.; Lo, K.; Russell, T. P.; Wang, L.; Liu, Y. *J. Am. Chem. Soc.* **2014**, *136* (42), 15093−15101.

(15) Noriega, R.; Rivnay, J.; Vandewal, K.; Koch, F. P. V.; Stingelin, N.; Smith, P.; Toney, M. F.; Salleo, A. *Nat. Mater.* **2013**, *12* (11), 1038−1044.

(16) Hendriks, K. H.; Li, W.; Wienk, M. M.; Janssen, R. A. J. *J. Am. Chem. Soc.* **2014**, *136* (34), 12130−12136.

(17) Bronstein, H.; Collado-Fregoso, E.; Hadipour, A.; Soon, Y. W.; Huang, Z.; Dimitrov, S. D.; Ashraf, R. S.; Rand, B. P.; Watkins, S. E.; Tuladhar, P. S.; Meager, I.; Durrant, J. R.; McCulloch, I. *Adv. Funct. Mater.* **2013**, *23* (45), 5647−5654.